INFECTION AND IMMUNITY, Dec. 2005, p. 8381–8392 Vol. 73, No. 12
0019-9567/05/$08.00+0 doi:10.1128/IAI.73.12.8381–8392.2005

Reduction of Cell Surface Glycosylphosphatidylinositol Conjugates in *Entamoeba histolytica* by Antisense Blocking of *E. histolytica* GlcNAc-Phosphatidylinositol Deacetylase Expression: Effect on Cell Proliferation, Endocytosis, and Adhesion to Target Cells

Divya Vats,[1] Ram A. Vishwakarma,[2] Sudha Bhattacharya,[3] and Alok Bhattacharya[1]*

School of Life Sciences, Jawaharlal Nehru University, New Delhi, India[1]; National Institute of Immunology, Aruna Asaf Ali Marg, New Delhi, India[2]; and School of Environmental Sciences, Jawaharlal Nehru University, New Delhi, India[3]

Received 23 May 2005/Returned for modification 2 July 2005/Accepted 6 August 2005

Glycosylphosphatidylinositol (GPI)-anchored molecules such as cell surface Gal/GalNAc lectin and proteophosphoglycans of the protozoan parasite *Entamoeba histolytica* are thought to be involved in pathogenesis. Here, we report the identification of genes that may be involved in the GPI biosynthetic pathway of *E. histolytica* by use of bioinformatic tools applied to the recently published genome sequence. Of the genes identified, one of the early genes, GlcNAc-phosphatidylinositol deacetylase (PIG-L), was partially characterized. Cell lines deficient in *E. histolytica* PIG-L (EhPL-AS) or overproducing it (EhPL-S) were generated by expressing the gene in the antisense or sense orientation, respectively, in a tetracycline-inducible system. The overexpressing cells showed higher EhPIG-L activity and increased production of GlcN-PI. Conversely, cells expressing the antisense RNA displayed reduced GlcN-PI production. The total number of GPI-containing molecules was also reduced in these cells, as demonstrated by Alexa 488 fluorescently labeled proaerolysin labeling. The distribution of GPI-linked PPG and Gal/GalNAc lectin was altered in the tetracycline-induced EhPL-AS cell lines. Further, the antisense-blocked cells showed 36% suppression of cell growth, 50 to 60% inhibition of fluid phase endocytosis, and about 50% inhibition of adhesion to target cells. Therefore, our data suggest the importance of GPI anchors in regulating some of the events in amoebic pathogenesis. They also demonstrated the use of antisense RNA-mediated inhibition of GPI biosynthetic enzymes as an approach to decrease the amount of GPI conjugates in *E. histolytica*.

The intestinal protozoan parasite *Entamoeba histolytica* is the causative agent of invasive amoebiasis, responsible for about 40,000 deaths every year (22, 40). Glycoconjugates and carbohydrate-binding proteins are involved in various disease pathologies, including amoebiasis. Attachment of *E. histolytica* trophozoites to target cells is required for cytolysis, and the process is thought to be mediated by the cell surface Gal/GalNAc lectin (44, 55). The glycocalyx layer on the surface of pathogenic *E. histolytica* trophozoites is predominantly made of proteophosphoglycan (PPG) (26, 41). No significant glycocalyx layer has been found on the surface of the nonpathogenic *Entamoeba dispar* (34). This correlates with the absence of PPG in *E. dispar* and suggests that PPG may have a role in pathogenesis (2, 3). Both Gal/GalNAc lectin and PPG are anchored to the plasma membrane by glycosylphosphatidylinositol (GPI) anchors and have been suggested to be good vaccine targets (19, 26). A number of reports emphasize the role of glycoconjugates in pathogenesis of other protozoan parasites (23, 36). For example, lipophosphoglycan (LPG) is the predominant molecule on the surface of *Leishmania* promastigotes and is known to be involved in pathogenesis (17, 32). Promastigotes deficient in GPI-anchored gp63 and LPG molecules displayed reduced virulence in terms of macrophage infectivity (24, 28, 51, 52). LPG facilitated promastigote attachment to the sandfly insect vector and provided resistance to complement-mediated lysis of metacyclic forms and may be essential for viability, replication, and/or virulence (24, 28, 33). GPI-deficient *Trypanosoma cruzi* amastigotes differentiated poorly to promastigotes and were inhibited in cellular growth (1). Malarial GPI molecules were found to be potent toxins closely associated with clinically severe malaria and capable of inducing cytokine and adhesin expression in macrophages and vascular endothelium (48). The glycan chain in the GPI was suggested to be a good vaccine candidate (47).

The Gal/GalNAc lectin of *E. histolytica* consists of two subunits (heavy and light), of which the light subunit is GPI anchored (29). There is also an intermediate form (IGL) of the lectin that colocalizes with the heavy and light subunits (10). The IGL is also anchored to the membrane through a GPI linkage. Cells expressing a dominant-negative form of the light subunit of Gal/GalNAc lectin (LGL) showed reduced cytolysis (21). Moreover, expression of truncated LGL molecules lacking the capability to have GPI anchors in *E. histolytica* cells also led to a reduction in virulence (30), suggesting that GPI anchors are important for lectin function and that the enzymes involved in GPI biosynthesis may be potential drug targets.

GPIs share a common core structure (28). Typically phosphatidylinositol (PI) is glycosidically linked to the reducing end of a nonacetylated glucosamine moiety, followed by three man-

* Corresponding author. Mailing address: School of Life Sciences, Jawaharlal Nehru University, New Mehrauli Road, New Delhi-110067, India. Phone: 91 11 26704516. Fax: 91 11 26717586. E-mail: alok0200@mail.jnu.ac.in.

nose residues which, in turn, are attached to ethanolamine linking the anchor to the protein destined to be GPI anchored (28). However, the GPI anchors in *E. histolytica* have a unique glycan backbone, that is, Gal-Man-Man-GlcN-myoinositol, with the terminal mannose being replaced by α-Gal, which is not found in any other eukaryotic GPI core structures reported so far (35). The biosynthesis of GPI anchors occurs in the endoplasmic reticulum and involves the stepwise assembly of the anchor on PI in the endoplasmic reticulum membrane (28). Though there are a few species-specific modifications in terms of the sequence of events, transfer of GlcNAc and deacetylation to form GlcN-PI appear to be the first two universal steps in the GPI biosynthesis (12, 18). The GPI-GlcNAc-transferase (GPI-Gnt) complex catalyzes the first step of the pathway, that is, transfer of GlcNAc from UDP-*N*-acetylglucosamine to PI. There are at least six subunits that make up the complex (58, 59, 61). On the other hand, a single polypeptide, PIG-L or GPI12 (*Saccharomyces cerevisiae*), carries out the deacetylation reaction (37, 55).

The enzymes of GPI anchor biosynthesis are thought to be excellent targets for chemotherapy in many parasite infections, and GPI anchors have also been targets of immunoprophylaxis (6, 26, 34, 47). Nothing is known about the GPI anchor biosynthetic pathway of *E. histolytica* and the enzymes that are involved. In this report, we have identified the various components of the pathway from sequence analysis of the *E. histolytica* genome database. Further, we have characterized GlcNAc-PI-deacetylase, the enzyme catalyzing the second step of GPI biosynthetic pathway, and generated cell lines that are partially blocked in this enzyme. These cells had an overall reduction of total GPI-containing molecules and were altered in many biological parameters, such as growth, adhesion, and endocytosis.

MATERIALS AND METHODS

Antibodies, strains and cell growth. Monoclonal antibody 2D7.10 was raised against the PPG of *E. histolytica* strain HM-1:IMSS (5). Monoclonal anti-Gal/GalNAc lectin 1D4 antibody (anti-LGL) was a kind gift of W. A. Petri (31).

All experiments were carried out with *E. histolytica* strain HM-1:IMSS clone 6, which was obtained from William A. Petri (University of Virginia). The cells were maintained and grown in TYI-33 medium supplemented with 15% adult bovine serum, 2% Diamond's vitamin mix, and antibiotic (0.3 units/ml penicillin and 0.25 mg/ml streptomycin). Hygromycin (Sigma) was added at 10 μg/ml for maintaining the transformed cell lines. Cell viability was determined by microscopy using a trypan blue dye exclusion test. Experiments were conducted with cells that showed >90% viability.

Sequence analysis. Amino acid sequences of genes involved in GPI anchor biosynthesis from various organisms were retrieved from the "PIGs Main" server (http://mendel.imp.univie.ac.at/sequences/gpi-biosynthesis/). Sequences that were not available at "PIGs Main" were identified using the NCBI database (http://www.ncbi.nlm.nih.gov). These were then used for BLAST analysis for a search of the *E. histolytica* genome database (12.5× coverage, that is, the final assembled genome sequence) at The Institute of Genome Research (http://www.tigr.org/tdb/e2k1/eha1), the Wellcome Trust's Sanger Institute (http://www.sanger.ac.uk/Projects/E_histolytica), and NCBI. The identified genes from the *E. histolytica* database were then further analyzed and confirmed by a number of search tools using a variety of databases such as reverse BLAST, PSI-BLAST, CD-search (http://www.ncbi.nlm.nih.gov/BLAST), Pfam (http://pfam.wustl.edu/hmmsearch.shtml), MPSrch (http://www.ebi.ac.uk/MPsrch), and ProDom (http://www.sanger.ac.uk/software/Pfam). The transmembrane prediction of the protein was made using various programs available at Bioinformatics.Net (http://www.bioinformatics.vg/biolinks/bioinformatics/transmembrane%2520domains.shtml). Determination of amino acid composition, translation of a given DNA sequence, and multiple alignments (CLUSTALW) were performed using the BioEdit sequence alignment editor (Tom Hall, version 7.0).

Metabolic labeling of cells. Mid-log-phase cells (2.5×10^5 cells/ml) were incubated with radiolabeled precursor *N*-acetyl-D-[1-^{3}H]glucosamine (Amersham Biosciences) (100 μCi/ml) in TYI-S-33 medium for indicated time periods. After incubation, the cells were harvested and washed twice with phosphate-buffered saline (PBS).

Preparation of amoebic crude membranes and total cell lysate. Membranes were prepared from *E. histolytica* as described previously by Carver and Turco (9). Briefly, 4×10^7 cells were resuspended in 10 ml of HEPES buffer (100 mM HEPES [pH 7.5], 50 mM KCl, 10 mM $MnCl_2$, 10 mM $MgCl_2$, 2 mM PMSF [phenylmethylsulfonyl fluoride], 5 to 10 μg/ml leupeptin) containing 10% glycerol and lysed by glass Dounce tissue homogenizer at 4°C. The debris and unbroken cells were removed by centrifugation at 250 × g for 5 min. The membrane fraction was collected by ultracentrifugation at 100,000 × g for 1 h at 4°C. The membrane pellet was washed once with reaction buffer (50 mM HEPES [pH 7.5], 5 mM EDTA, 1 μg/ml leupeptin, 2 mM PMSF) without glycerol and finally resuspended in the same buffer.

Total cell lysate was prepared as described previously (4). Briefly, the cells were harvested and washed thrice with PBS. The cells were then lysed by hypotonic shock (10 mM Tris-Cl [pH 7.5], 2 mM PMSF, 1 mM PHMB [*p*-hydroxymercuribenzoate], 4 g/ml leupeptin) for 10 min. After three cycles of freezing and thawing at −70°C and 37°C, respectively, DNA was sheared by sonicating thrice for 15 s. The lysate was stored as aliquots at −70°C.

In vitro synthesis of GPI pathway intermediates. Radiolabeled GPI intermediates were synthesized in vitro by incubating *E. histolytica* crude membrane preparation (typically 1 mg protein) with UDP-[^{14}C]GIcNAc (0.05 μCi) (Amersham Biosciences) in reaction buffer in a total volume of 200 μl. After incubation at 37°C for 2 h, the reaction was stopped by incubating on ice. The labeled products were extracted first by shaking with 600 μl water and 3 ml ice-cold chloroform-methanol (1:2 [vol/vol]) followed by addition of 1 ml each of chloroform and water. The mixture was centrifuged at 1,000 × g for 10 min at 4°C in order to separate the phases. The lipid containing the chloroform-rich lower phase was washed twice with 0.5 ml mock upper phase to remove any contaminating UDP-[^{14}C]GlcNAc or breakdown products. Then, 10% of the lipid-containing phase was taken for liquid scintillation counting. The remainder of the sample was dried, dissolved in 20 μl water-saturated butanol (w-butanol), and analyzed by high-performance thin-layer chromatography (HPTLC). HPTLC plates (Merck) were developed using chloroform–methanol–1 M ammonium hydroxide (10:10:2 [vol/vol/vol]) as the solvent system. The plates were air dried to remove any traces of ammonia followed by spraying with EN^{3}HANCE (NEN Life Science) for fluorography.

Characterization of GPI pathway intermediates. (i) Phenyl Sepharose chromatography. The extracted glycolipids were loaded on a 1 ml phenyl Sepharose column equilibrated with 100 mM ammonium acetate–5% 1-propanol in water (solvent A). A gradient was set up with various concentrations of solvent A and solvent B (60% 1-propanol in water) at a flow rate of 4 ml/h. Then, 1-ml fractions were collected and the amount of radioactive material in each fraction was determined by liquid scintillation counting.

(ii) Enzymatic cleavage of glycolipids by PI-PLC treatment. Purified phosphatidylinositol-specific phospholipase C (PI-PLC) was obtained from Martin Low (Columbia University College of Physicians and Surgeons, New York, N.Y.). Radiolabeled products were treated with 0.1 U/ml of PI-PLC at 37°C for indicated time periods, and the lipids were extracted as described above and analyzed by HPTLC followed by fluorography.

(iii) Acetylation. The dried sample ([^{14}C]-labeled glycolipids) was resuspended in 50 μl of saturated sodium bicarbonate, and 2 μl of acetic anhydride was then added. After 30 min of incubation on ice another 3 μl of acetic anhydride was added. The reaction mixture was further incubated at 20°C for 30 min. Acetylated glycolipids were extracted using w-butanol. The reaction mixture was again washed with butanol, and the butanol phases were pooled and dried. The dried acetylated product was resuspended in w-butanol and analyzed by HPTLC as mentioned above.

(iv) Nitrous acid deamination. A total of 250 μl of freshly prepared 0.4 M $NaNO_2$ (pH 5.5) was added to the dried [^{14}C]-labeled glycolipids. The pH of the reaction was adjusted to 3.5 to 4.0 using acetic acid, and then the reaction mixture was incubated for 4 h. Further, 50 μl of freshly prepared 1 M $NaNO_2$ was added and incubation was continued for another 8 h at room temperature. The reaction was terminated by adding 250 μl of w-butanol, and the reaction mixture was mixed and then centrifuged for phase separation. The upper butanol phase was removed, and the lower phase was reextracted with w-butanol. All the butanol phases were pooled and dried using vacuum and then resuspended in 20 μl of the same solvent. Deaminated glycolipids were subjected to HPTLC analysis.

TABLE 1. Putative GPI biosynthetic pathway enzymes of *E. histolytica*, yeast, and humans

Enzyme	Human gene	*S. cerevisiae* gene	*E. histolytica* gene	Accession no./genomic locus of *E. histolytica* genes
GPI-GlcNAc-transferase complex (GPI-GnT complex)	PIG-A	GPI3	EhPIG-A	EAL51260/AAFB01000048
	PIG-C	GPI2	EhPIG-C	EAL48156/AAFB01000298
	PIG-H	GPI15	ND[a]	
	PIG-P	PIG-P	EhPIG-P	EAL47301/AAFB01000388
				EAL47099/AAFB01000406
				EAL47075/AAFB01000408
				EAL43001/AAFB01001119
	PIG-Q	GPI1	EhPIG-Q	EAL49884/AAFB01000136
	DPM2	ND	ND	
GPI-deacetylase	PIG-L	GPI-12	EhPIG-L	EAL49111/AAFB01000209
MTI	PIG-M	GPI10	EhPIG-M	EAL44694/AAFB01000708
				EAL47045/AAFB01000410
MTII	PIG-X	Pbn1p	EhPIG-X	EAL43352/AAFB01001009
				EAL49190/AAFB01000202
MTIII	PIG-V	GPI18	EhPIG-V	EAL48755/AAFB01000238
	PIG-B	GPI14	ND	
MTIV	SMP3	SMP3	ND	
Dol-P-man-synthase	DPM1	DPM1	EhDPM1	EAL46013/AAFB0100
Phosphoethanolamine transferase complex	PIG-N	MCD4	ND	
	GPI7	GPI7	ND	
	PIG-O	GPI13	EhPIG-O	EAL47397/AAFB01000376
	PIG-F	GPI11	ND	EAL50726/AAFB01000082
GPI-transamidase complex	GPAA1	GAA1	ND	
	PIG-K	GPI8	EhPIG-K	EAL49152/AAFB01000205
	PIG-S	GPI17	EhPIG-S	EAL47456/AAFB01000369
	PIG-T	GPI16	EhPIG-T	EAL47777/AAFB01000333
	PIG-U	Cdc91p	EhPIG-U	EAL44658/AAFB01000711
				EAL47069/AAFB01000408
GPI-deacylase	PIG-W	GWT1	EhPIG-W	EAL48691/AAFB01000242

[a] ND, not detected.

Northern hybridization. Total RNA was purified using TriPure reagent (Roche Applied Science) according to the manufacturer's instructions. RNA samples (30 μg) were denatured and size fractionated in a 1.2% formaldehyde gel in 1× formaldehyde gel running buffer. The gel was processed using standard molecular biology protocols and blotted onto a GeneScreen Plus nylon membrane (NEN). It was hybridized with denatured radiolabeled probe in salmon sperm DNA (100 μg/ml) according to the manufacturer's instructions. Radiolabeled probes were prepared by using either random primers (for labeling double-stranded probe) or strand-specific primers (for single-stranded probe) for a DNA probe complementary to *E. histolytica* PIG-L (EhPIG-L) antisense RNA. The double-stranded probe used was a 0.734-kb fragment containing the complete coding region of EhPIG-L (double stranded); for identifying PIG-L antisense RNA, the strand-specific primer 5′-GGG GGA TCC CAT ATG GCT GAA GCA CT-3′ (PLAS-F) was used (single stranded).

PCR. Primers to amplify the EhPIG-L open reading frame were designed based on sequences in the *Entamoeba* GSS sequence database. Appropriate restriction enzyme sites were incorporated in the primers used for PCR amplification of the coding region of the EhPIG-L gene. The antisense forward and reverse primers used were 5′-GCG GGA TCC TCA CGA ATG TCT AGT ACA ACA AT-3′ (PLAS-F) and 5′-GCG GGT ACC GTA ATA TTC AAC TAA TTG ATT TAA-3′ (PLAS-R). The sense forward and reverse primers were 5′-GCG GGT ACC TCA CGA ATG TCT AGT ACA ACA AT-3′ (PLS-F) and 5′-GCG GGA TCC GTA ATA TTC AAC TAA TTG ATT TAA-3′ (PLS-R). Total genomic DNA was purified from late-log-phase-grown cells as described earlier, and 200 ng of this DNA was used for PCR (7). The PCR conditions were 92°C for 7 min; 37°C for 1 min; 70°C for 1 min; 92°C for 30 s (5 cycles); 42°C for 1 min; 70°C for 1 min; 92°C for 30 s (25 cycles); 42°C for 1 min; and 70°C for 1 min (1 cycle). The PCR products were cloned in pGEMT-easy vector (Promega) and subsequently in pEhHYG-tetR-O-CAT (15). The chloramphenicol acetyltransferase (CAT) gene was excised using KpnI and BamHI restriction endonucleases, and the PIG-L gene was inserted in either the sense or the antisense orientation. Plasmids containing PIG-L gene in sense and antisense orientations were constructed and named pEhPL-S and pEhPL-AS, respectively. The cell lines generated with parental vector (pEhHYG-tetR-O-CAT), pEhPL-S, and pEhPL-AS constructs are referred to as vector, EhPL-S, and EhPL-AS, respectively.

PLS-F and PLS-R primers were used to amplify reverse-transcribed products obtained from total HM1:IMSS RNA (5 μg) under similar conditions, using standard molecular biology protocols (46).

Transfection of *E. histolytica* trophozoites by electroporation. Transfection was performed by electroporation as described previously (15, 60). Two consecutive pulses were applied instead of one pulse, each with an exponential discharge of 3,000 V/cm at a capacitance of 25 μF (Gene Pulser II; Bio-Rad). For each transfection 1×10^7 trophozoites and 300 μg DNA were used. Drug selection with 10 μg/ml hygromycin (Sigma) was started 48 h after transfection.

Immunostaining. *E. histolytica* cells (2×10^5) resuspended in incomplete TYI-33 medium at 36°C were transferred onto coverslips placed in a petri dish and allowed to adhere for 10 min at 36°C, and cells were fixed with 3.7% prewarmed paraformaldehyde for 30 min at 36°C. After fixation, the cells were permeabilized with 0.1% Triton X-100–PBS for 1 min and then quenched with 50 mM NH_4Cl–PBS for 30 min. The coverslips were blocked with 1% bovine serum albumin (BSA)–PBS for 30 min, followed by incubation with monoclonal antibody for 1 h at 36°C. These were first washed with PBS and then with 1% BSA–PBS before incubation with secondary antibodies at a 1:200 dilution for 30 min at 36°C. The combinations of antibodies used were monoclonal antibody 2D7.10 (anti-PPG) at 1:100 along with cy3-labeled anti-mouse immunoglobulin G (IgG) and monoclonal anti-Gal/GalNAc lectin antibody 1D4 (anti-LGL) at 1:30 in combination with Alexa-488-labeled anti-mouse IgG at 1:200 dilution. The preparations were further washed with PBS and mounted on a glass slide using DABCO [1,4-diazbicyclo(2,2,2)octane] (Sigma) (10 mg/ml) in 80% glycerol and sealed. Cy3-labeled and Alexa-488-labeled cells were visualized using a laser scanning confocal microscope (FV300 Olympus) after excitation at 543 nm and 488 nm, respectively.

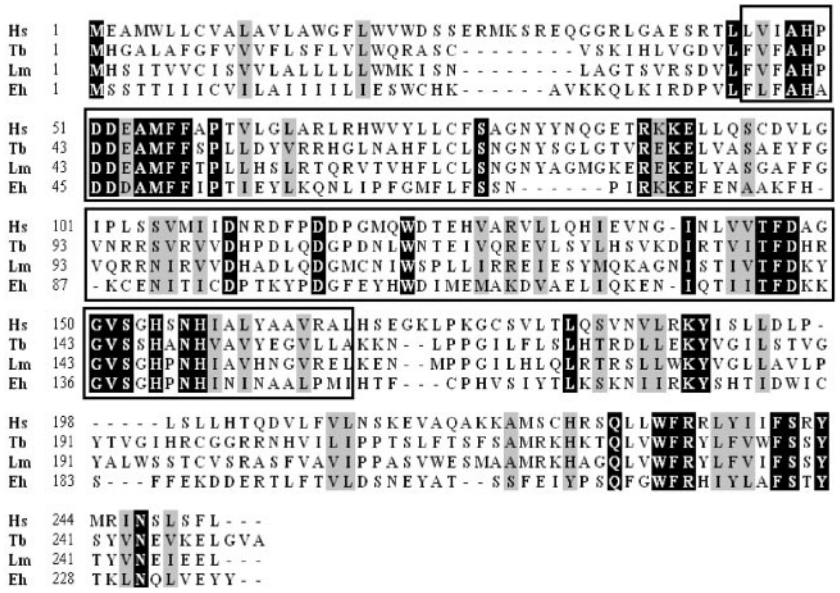

FIG. 1. The EhPIG-L gene of *E. histolytica*. ClustalW alignment of EhPIG-L protein (Eh) with those of *Leishmania* (Lm), *Trypanosoma* (Tb), and human (Hs) homologs, respectively. The boxed regions show a conserved Pfam domain (PF02585) common to all PIG-L proteins. Black- and gray-shaded regions indicate identical and similar amino acids. Amino acid positions are indicated on the left.

FLAER labeling to map GPI conjugate. Proaerolysin is a nontoxic precursor of a 47-kDa channel-forming protein aerolysin and is generated by proteolytic processing. The binding of proaerolysin to lipid bilayers was studied with Alexa 488-labeled proaerolysin (fluorescently labeled proaerolysin [FLAER]), and the labeled cells were analyzed by confocal microscopy (8). Briefly, *E. histolytica* cells (1×10^5) were harvested and resuspended in incomplete TYI-33 medium. These were then incubated with 10^{-8} M FLAER (Protox Biotech) at 20°C for 1 h. The cells were washed with PBS to remove unbound FLAER and fixed in 3.7% paraformaldehyde for 30 min at 36°C. The labeled cells were visualized using a laser scanning confocal microscope after excitation at 488 nm.

Cellular proliferation. *E. histolytica* cells transfected with pEhPL-AS and parental vector were grown in the presence of 10 μg/ml hygromycin B, and the growth was measured in the absence and the presence of 10 μg/ml tet after 72 h. The cells were counted with a hemocytometer. Cell viability was determined by microscopy using a trypan blue dye exclusion test.

FITC-dextran uptake analysis. The endocytosis in *E. histolytica* was studied by observing the uptake of fluorescein isothiocyanate (FITC)-dextran. The mid-log-phase cells were harvested, washed, and resuspended in PBS. The cells were incubated with FITC-dextran (FD-40; Sigma) (2 mg/ml) for 30 min at 36°C. The slides were visualized under a fluorescent microscope (Axioscope plus; Zeiss). The amount of FITC-dextran uptake was determined by first lysing the FITC-dextran containing trophozoites in PBS containing 0.1% nonionic detergent (Nonidet) NP-40 and then measuring fluorescence emission at 520 nm, using a fluorescence spectrophotometer (Varion; Cary) with the excitation wavelength at 485 nm.

Target cell adherence assays. (i) Adherence to CHO cells. Rosette formation was assayed as described previously (43). Briefly, *E. histolytica* (1×10^3) and CHO (2×10^4) cells were mixed in 1 ml of TYI-S-33 medium and then centrifuged at $150 \times g$ for 5 min. The amoeba and CHO cell pellet was transferred to 24-well culture plates and further coincubated for 2 h with gentle shaking. *E. histolytica* cells with at least three adhered CHO cells (referred to as an amoeba-CHO cell rosette) were counted under an inverted light microscope (Nikon) at ×40 magnification.

(ii) Adherence to HRBCs. Fresh human erythrocytes (HRBCs) were obtained from healthy donors and were washed with PBS and centrifuged. The pellet was resuspended in TYI-S-33 medium. Amoeba and HRBCs were coincubated together at a 1:20 ratio, and adherence was calculated as described earlier for CHO cells.

Miscellaneous methods. The concentration of protein in a sample was estimated using an bicinchoninic acid assay with BSA as a standard (50). The paired *t* test was used to calculate the statistical significance of any differences between the experimental groups. Statistical significance was set at $P < 0.05$.

RESULTS

GPI anchor biosynthetic pathway genes in *E. histolytica*. The biosynthesis of GPI anchors is a multistep process involving many intermediates. A number of enzymes and enzyme complexes participate in these steps leading to the synthesis of GPI-anchored molecules. Data from other biological systems suggest the presence of at least 10 reaction steps for the GPI core biosynthesis, and more than 20 genes may be involved in this pathway (13).

In an effort to understand and elucidate the GPI biosynthesis pathway in *E. histolytica* we undertook a detailed computational analysis of the *E. histolytica* genome (12.5× coverage) (25). Using the amino acid sequences of known genes of GPI biosynthesis pathway from other organisms such as yeast and humans and *Leishmania* and *Trypanosoma* spp. as queries, we searched for their corresponding homologues in *E. histolytica*. The hits were considered significant when the maximum e-value obtained in the BLAST analysis was 0.00001. Some of the hits were also confirmed by the presence of motifs or of demonstrated similarity with protein families by use of "Prosite" and "Pfam." Out of a total of 22 genes in yeast and 23 in humans only 15 genes were identified in *E. histolytica* (Table 1). It is difficult to say at present whether homologs of proteins present in other organisms and not found in *E. histolytica* are missing or have diverged significantly so that these are not detectable in spite of the use of sensitive search methods. Interestingly, the proteins that were found to be absent in *E. histolytica* by database search were not the catalytic subunits of multienzyme complexes (Table 1). It appears from these data that the GPI biosynthetic pathway of *E. histolytica* is likely to be substantially different from that present in other organisms. Since the deacetylase activity is carried out by a single subunit

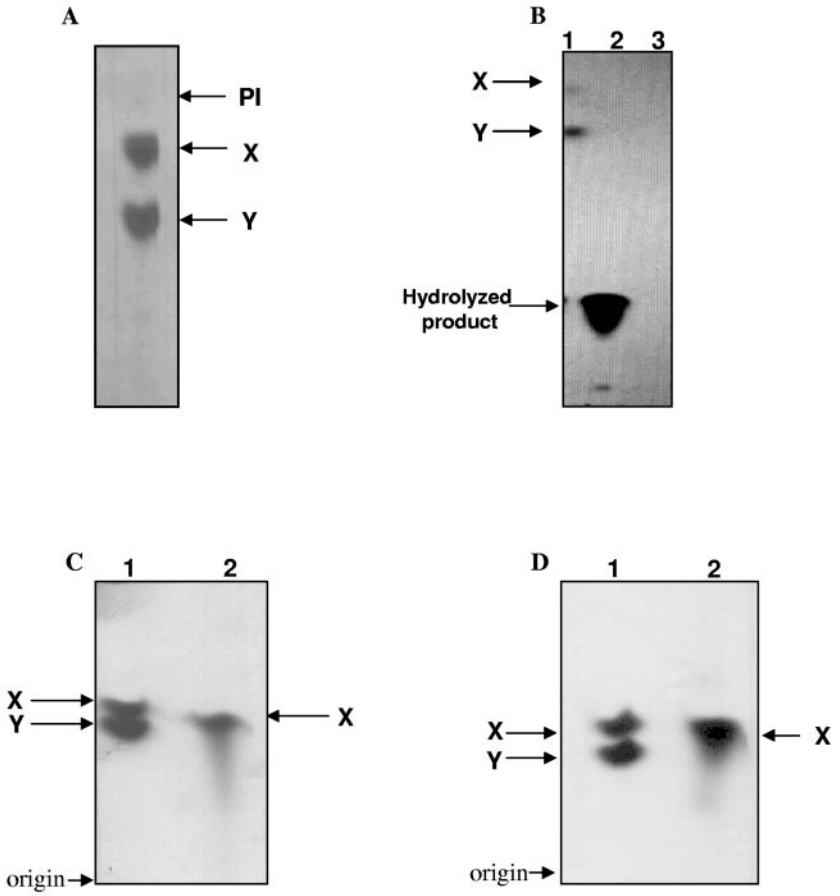

FIG. 2. Cell-free biosynthesis of GPI intermediates and their characterization. (A) HPTLC profile of in vitro reaction products. *E. histolytica* crude membranes (2×10^7 cells) were incubated with UDP-[^{14}C]GlcNAc (0.05 μCi) in reaction buffer and analyzed by HPTLC as described in Materials and Methods. Two major radiolabeled products, X and Y, were identified by fluorography. The position of PI is indicated by an arrow. (B) PI-PLC hydrolysis of products shown in panel A. Lane 1, untreated intermediates (R_f values: X = 0.78; Y = 0.72); lane 2, PI-PLC-hydrolyzed products in aqueous phase (R_f value = 0.3); lane 3, PI-PLC-hydrolyzed products in organic phase. (C) Nitrous acid deamination. Radiolabeled glycolipid products of in vitro reactions were subjected to nitrous acid deamination followed by HPTLC analysis and fluorography. Lane 1, untreated sample; lane 2, HNO_2-treated sample. (D) Acetic anhydride acetylation. HPTLC profile of radiolabeled glycolipids after *N* acetylation by acetic anhydride. Lane 1, untreated glycolipids; lane 2, acetic anhydride-treated glycolipids.

encoded by PIG-L, we subsequently focused our studies on this gene.

Sequence analysis of EhPIG-L gene. The putative *E. histolytica* EhPIG-L gene (EAL49111.1) showed 33% identity and 47.5% similarity with the human PIG-L gene. *E. histolytica* PIG-L encodes a putative protein of 237 amino acids, with a predicted size of about 27 kDa. ClustalW alignment with the proteins from human and other protozoan parasites showed significant regions of conservation dispersed over the length of the protein (Fig. 1). A conserved Pfam domain (accession number PF02585) common to all PIG-L orthologs was also found in EhPIG-L spanning amino acid positions 39 to 154.

GlcNAc-PI-deacetylase activity in *E. histolytica* membrane vesicles. Data presented in the previous section showed the presence of a putative GlcNAc-PI-deacetylase gene in the *E. histolytica* genome. In order to show whether such an activity exists in these cells, biochemical assays were performed for the first two enzymes, namely, GPI-*N*-acetylglucosamine transferase (GPI-Gnt complex) and GlcNAc-PI-deacetylase (PIG-L), in a cell-free system containing microsomal membranes (9). The cell-free system was incubated with UDP-[^{14}C]GlcNAc, and the products were analyzed by HPTLC as described in Materials and Methods. The products resolved into two major radiolabeled products, X and Y, which migrated slower than PI (Fig. 2A). The products (X and Y) migrated with R_f values of 0.76 and 0.72, respectively. The values were found to be similar to those of GlcNAc-PI and GlcN-PI as reported for other organisms, such as mammals, yeast, and *Leishmania* spp.

In order to show that the reaction products were indeed GlcNAc-PI and GlcN-PI, further analysis was carried out. The radiolabeled reaction products bound phenyl Sepharose and were found to elute at 30% *n*-propanol, a property typical of many GPI-anchored molecules (references 9 and 14 and data not shown). The reaction products were susceptible to PI-PLC hydrolysis (Fig. 2B). About 85% of the material was digested within 1 h when incubated with 0.1 U/ml of PI-PLC (data not shown). Since the bulk of the radioactivity released was in the aqueous phase migrating near the origin (Fig. 2B, Lane 2), it suggested that a glycan group may have been generated after

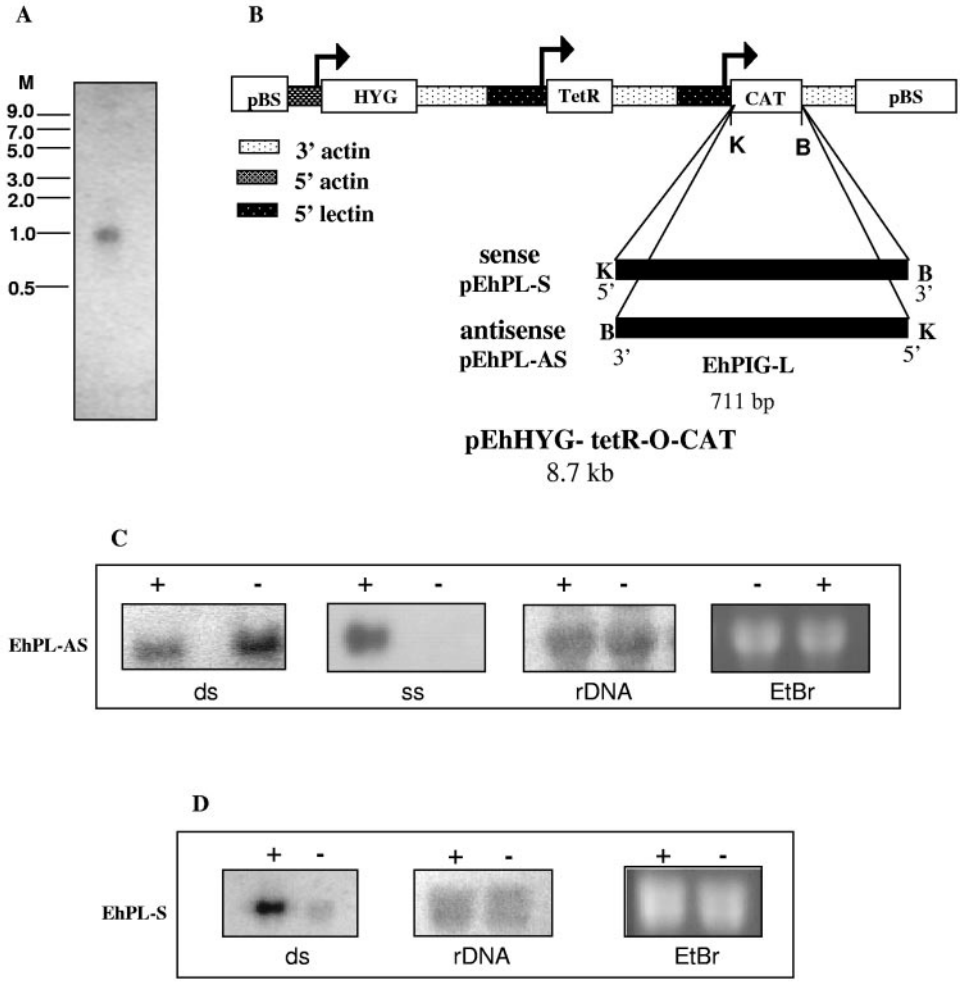

FIG. 3. Expression of EhPIG-L in cultured and transformed *E. histolytica* cells. Total RNA was extracted from trophozoites of *E. histolytica*, and 30 μg was used for Northern analysis as described in Materials and Methods. (A) Endogenous expression of EhPIG-L in cultured *E. histolytica* cells. The blot was hybridized with the full-length coding region of EhPIG-L. Molecular mass markers are in kilobase pairs. (B) Schematic description of a plasmid pEhHYG-tetR-O-CAT. The CAT gene of the *E. histolytica* shuttle vector pEhHYG-tetR-O-CAT was excised using KpnI and BamHI. The EhPIG-L gene was inserted in its place in either the sense (pEhPL-S) or the antisense (pEhPL-AS) orientation. Northern analysis of RNA was performed using the cell lines transformed with pEhPL-AS (C) and pEhPL-S (D), and the blots were hybridized under stringent conditions with single-stranded DNA probe complementary to EhPIG-L antisense-RNA (ss) and a double-stranded EhPIG-L probe (ds). For probing antisense RNA, specific primer PLAS-F was used. *E. histolytica* rRNA gives two bands at 1.6 kb and 1.9 kb, respectively. K, KpnI, B, BamHI; HYG, 1 kb, TetR, 0.61 kb, CAT, 0.65 kb, pBS, 3.19 kb.

the digestion. Both the products were susceptible to digestion by the enzyme (Fig. 2B, lane 3).

The susceptibility to nitrous acid deamination is also a diagnostic feature of a GPI-anchored molecule. After nitrous acid deamination, the glycolipids labeled in vitro were hydrolyzed, as revealed by loss of product Y only, unlike the results seen with PI-PLC treatment (Fig. 2C). This showed that one of the products (Y) contains a PI anchor with a free amine, which may have been generated through a deacetylation reaction.

In order to conclusively show the identity of the deacetylated intermediate, reaction products were subjected to *N*-acetylation by acetic anhydride. This would convert GlcN-PI to GlcNAc-PI, which would be reflected in the shifting of the position in HPTLC. Y was found to comigrate with X after acetylation, indicating that X was the acetylated derivative of Y (Fig. 2D). These observations confirmed that the products X and Y were GlcNAc-PI and GlcN-PI, respectively.

Molecular characterization of EhPIG-L gene. The nucleotide sequence of the predicted gene, EhPIG-L, was used to design PCR primers PLS-F (forward) and PLS-R (reverse), and the PCR amplicon was cloned and sequenced. The endogenous expression of the gene in *E. histolytica* was examined by Northern blotting. A single transcript of about 0.9 kb was observed in Northern blot analysis (Fig. 3A). The extra nucleotides in the transcript compared with the coding region may be contributed by untranslated regions and a poly(A) tail. Reverse transcription-PCR also showed the presence of a band of expected size (data not shown). These results suggested that the putative PIG-L of *E. histolytica* is expressed in trophozoites.

Inducible expression of PIG-L. A tetracycline-inducible gene expression system for *E. histolytica* was reported previously (45). Molecular cloning of the PIG-L gene in pEh-HYG-tetR-O-CAT vector has been described in Materials and Methods and is schematically shown in Fig. 3B.

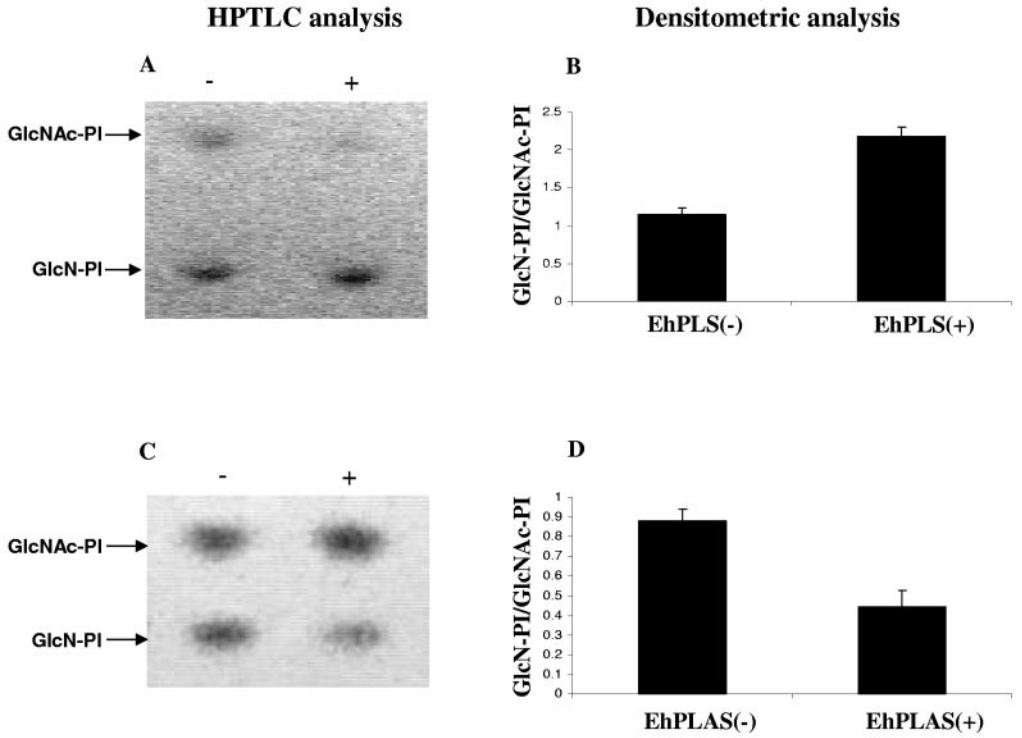

FIG. 4. GlcN-PI and GlcNAc-PI synthesis in EhPIG-L antisense (EhPL-AS) and EhPIG-L sense (EhPL-S) cells. Crude membranes were prepared from cells grown in the absence (−) and the presence (+) of tet. The cell-free assay was carried out as described earlier using 0.8 mg of respective membrane preparation. Glycolipids were extracted, and equal amounts of radioactivity (20,000 to 30,000 cpm for the different experiments) were used for HPTLC analysis followed by fluorography. The histogram represents the product-to-substrate ratio (GlcN-PI/GlcNAc-PI), based on four separate experiments. (A) HPTLC profile of EhPL-S cells, in the absence (−) and the presence (+) of tet. (B) Densitometric analysis of radiolabeled glycolipids extracted from EhPL-S cells for uninduced (−) and induced (+) states. (C) HPTLC profile of EhPL-AS cells, in the absence (−) and the presence (+) of tet. (D) Densitometric analysis of glycolipids extracted from EhPL-AS cells for uninduced (−) and induced (+) states.

In order to determine expression levels of EhPIG-L in overexpressing (EhPL-S) and antisense-blocked (EhPL-AS) cells, Northern hybridization of EhPIG-L was carried out using the entire EhPIG-L coding region in the presence and the absence of tetracycline. In EhPL-AS cells a high level of expression of antisense PIG-L was observed in the presence of tet (Fig. 3C; ss). However, there was a twofold reduction in EhPIG-L transcripts in EhPL-AS cells when the double-stranded gene was used in Northern analysis (Fig. 3C; ds). There was a fivefold increase in the expression of the PIG-L gene upon addition of 10 μg/ml tet for 72 h in EhPL-S cells (Fig. 3D; ds). The results demonstrated the usefulness of the tet-regulated system for conditional expression of a gene in *E. histolytica* and showed that EhPIG-L expression can be down regulated in EhPL-AS cells upon addition of tet.

The transformed cell lines were further characterized biochemically by use of the cell-free system described earlier (58) to analyze the activities of GPI-Gnt complex and PIG-L. Equal amounts of extracted radiolabeled glycolipids (20,000 to 30,000 for different experiments) were subjected to HPTLC analysis. The ratio of the two products, namely, GlcNAc-PI and GlcN-PI, is indicative of the amount of PIG-L present in the cells. Extracts from EhPL-S cells grown in the presence of tet showed an accumulation of radioactive GlcN-PI and a reduction in GlcNAc-PI levels (Fig. 4A). The ratio of GlcN-PI to GlcNAc-PI was found to be 1.14 and 2.18 in the absence and the presence of tet, respectively, in a typical experiment (Fig. 4B). These experiments were repeated a number of times ($n = 4$); there was a statistically significant difference (P value < 0.05) in the ratio of GlcN-PI to GlcNAc-PI in the presence and the absence of the inducer. This result is expected if the putative gene codes for PIG-L enzyme whose levels rise in cells in the presence of tet. The converse is expected from EhPL-AS cells, where tet induction would lead to production of antisense RNA and thus inhibition of gene expression (Fig. 4C). In these cells the ratios of GlcN-PI to GlcNAc-PI were found to be 0.882 and 0.445 before and after tet induction, respectively, suggesting an increase in acetylated product (Fig. 4D).

The level of GPI-containing molecules. Aerolysin and proaerolysin have been shown to bind with high affinity to GPI-anchored molecules on the cell surface and therefore can be used to map GPI anchors quantitatively (8). The binding of proaerolysin to lipid bilayer was studied with FLAER, and the labeled cells were analyzed by confocal microscopy as described in Materials and Methods. This analysis indicated that there was a reduction of 85 to 90% in the number of fluorescent foci upon tet induction of EhPL-AS cells (Fig. 5A). The cells containing the parental vector showed no statistically significant change in labeling in the presence of tet (Fig. 5B). This indicated that the antisense RNA-mediated blocking of EhPIG-L gene expression led to a reduction in the amount of GPI-containing molecules on the amoebic cell surface.

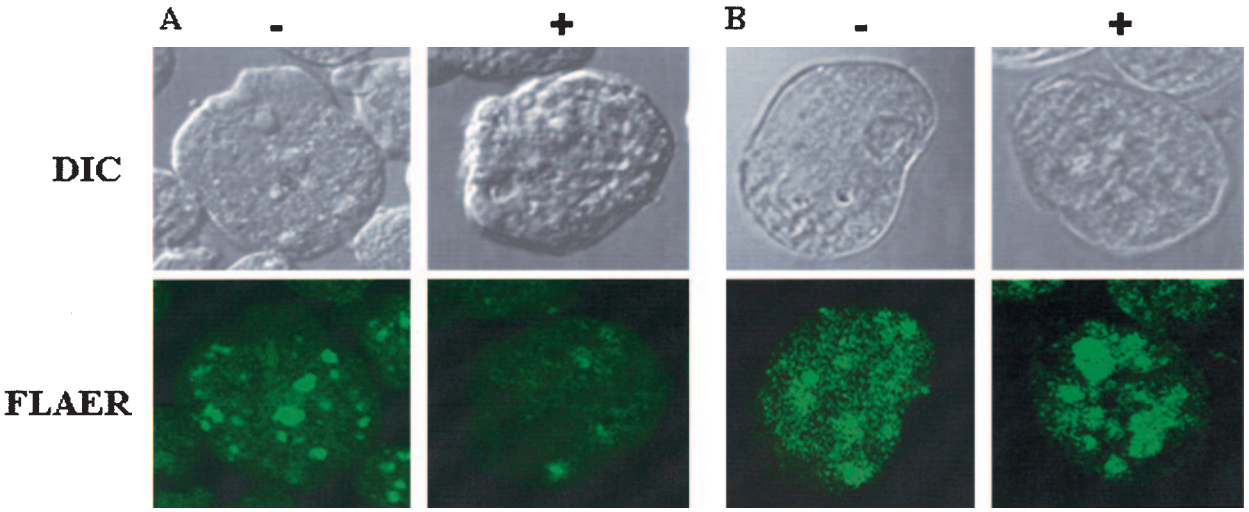

FIG. 5. Labeling of cell surface GPI-linked molecules by FLAER. EhPL-AS cells (2×10^5) were incubated with 10^{-8} M FLAER for 1 h at 20°C. The cells were then centrifuged and washed with PBS to remove unbound FLAER and subsequently fixed in 3.7% paraformaldehyde for 30 min at 37°C. The washed cells were resuspended in PBS and mounted on slides using 10 mg/ml DABCO in 80% glycerol. The fluorescent samples were examined on a laser-scanning confocal microscope (FV300 Olympus, Japan) equipped with a 60× objective. FLAER-labeled samples were visualized after excitation at 488 nm. (A) EhPL-AS cells, in the absence (−) and the presence (+) of tet. (B) Vector cells, in the absence (−) and the presence (+) of tet. DIC, differential interference contrast.

The expression of GPI-containing PPG and the small subunit of Gal/GalNAc lectin were studied in EhPL-AS cells by confocal fluorescence microscopy after immunostaining. The images are shown in Fig. 6. PPG was found mainly on the cell surface, and a uniform distribution was observed on EhPL-AS cells in the absence of tet (Fig. 6A, PPG). However, after induction most of the stained material was in the intracellular vacuoles and not on the cell surface (Fig. 6B, PPG). The specific staining of Gal/GalNAc lectin revealed a pattern of granular distribution spread over the cell as observed previously for the lectin (21). After tet induction the level of staining was also reduced significantly, but its distribution seemed to be unaffected (Fig. 6C and 6D; LGL). It appears from these results that there is a reduction in the number of GPI molecules in EhPIG-L expression-blocked cells.

Functional characterization of transformed cells. Cell proliferation is one of the key indicators of an altered cell physiology. Cell proliferation was determined in relation to antisense PIG-L expression. Cell number of EhPL-AS cells was found to decrease by 31 to 36% (P value < 0.01) in different experiments in the presence of tet for 72 h (Fig. 7A). No significant change was observed in cell proliferation when a control cell line carrying the parental vector was used.

In order to investigate the role of GPI-anchors in cytoadhesion, an assay involving binding of transformed *E. histolytica* trophozoites to CHO and HRBCs was performed. There was a 40% reduction in adherence of both CHO cells and HRBCs to EhPL-AS cells in the presence of tet compared to the results seen with cells grown without tet or the cells carrying the parental vector in the presence of the inducer (Fig. 7B). The quantum of reduction differed from experiment to experiment, ranging from 40 to 60%. This result suggests that GPI anchors are important for amoebic adhesion, as already known for one of the GPI conjugates in *E. histolytica* (Gal/GalNAc lectin).

The level of endocytosis was measured by determining the uptake of FITC-dextran. The level of FITC-dextran uptake in tet-induced EhPL-AS cells was found to be reduced by 50 to 60% compared to uninduced cell results. The cells containing vector alone did not show any significant change in uptake in the presence or the absence of the inducer (Fig. 7C). Fluorescent microscopic analysis of the cells showed similar results. The number of fluorescent pinocytic vesicles was reduced in EhPL-AS cells in the presence of tet (Fig. 7C). The results suggested that the level of endocytosis is reduced by antisense inhibition of PIG-L gene expression.

DISCUSSION

GPI-anchored molecules are involved in important processes in a variety of cell types and organisms. The amount and type of such molecules differ in different organisms, being less abundant in mammalian cells than in yeast and protozoa. Interestingly, GPI-anchored molecules in some of these organisms are thought to be involved in parasitism and pathogenesis (23, 36). The two major GPI-anchored cell surface molecules of *E. histolytica*, PPG and Gal/GalNAc lectin, are thought to be

FIG. 6. Immunostaining of PPG and Gal/GalNAc lectin in EhPL-AS cells. Trophozoites grown for 72 h were transferred to prewarmed, acetone-washed coverslips for 10 min at 36°C. The cells were then fixed with paraformaldehyde-PBS and permeabilized with 0.1% Triton–PBS followed by immunostaining with indicated antibodies. The stained cells were then visualized after excitation at 543 nm (for Cy3) and 488 nm (for Alexa-488) on a confocal laser scanning microscope (FV300 Olympus, Japan) equipped with a 60× objective. Panels A and B were stained with monoclonal anti-PPG antibody 2D7.10 followed by cy3-labeled anti-mouse IgGs, whereas panels C and D were stained with monoclonal anti-Gal/GalNAc lectin antibody 1D4 followed by Alexa488-labeled anti-mouse IgGs. Panels A and C show uninduced cells; panels B and D show tet-induced cells. DIC, differential interference contrast.

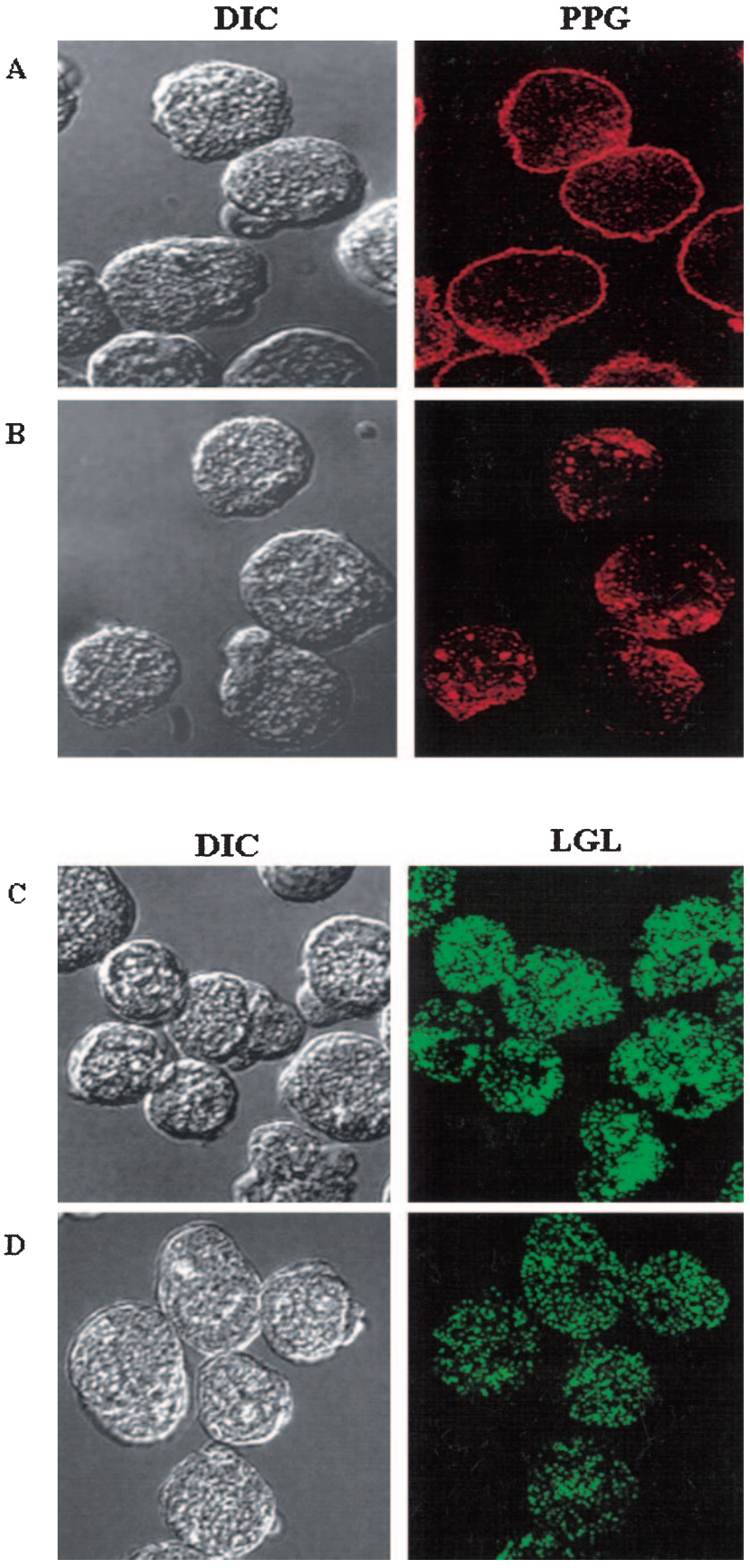
DIC
PPG
A
B
DIC
LGL
C
D

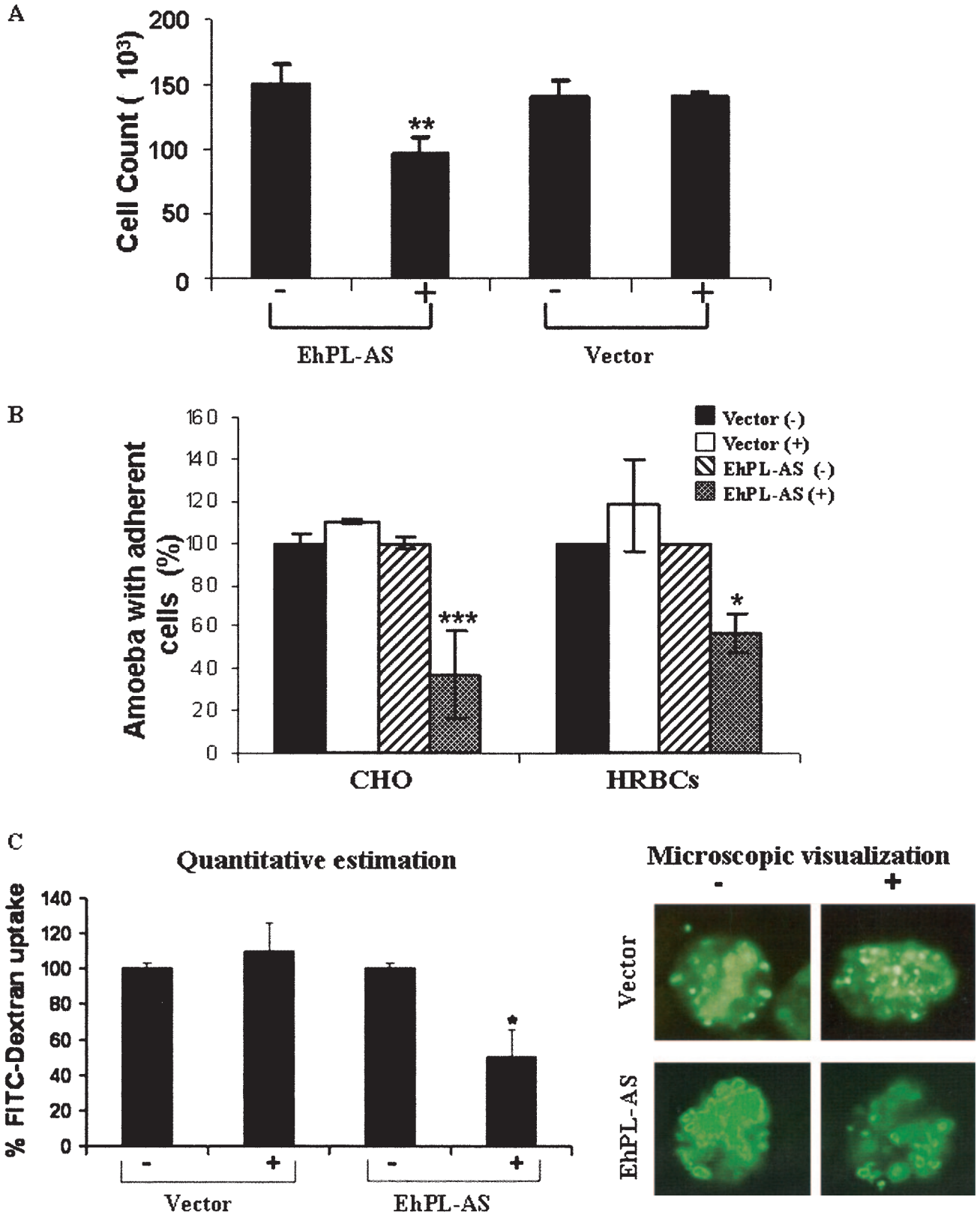

FIG. 7. Functional characterization of pEhPL-AS-transformed cells. (A) Growth of cell lines transfected with pEhPL-AS and vector constructs. All cells were grown in the presence of 10 μg/ml hygromycin B, and growth was measured in the absence and the presence of tet for 72 h. (B) Target cell adherence. An adherence assay was performed as described in Materials and Methods. *E. histolytica* cells were incubated with target cells, and the numbers of amoebae with three or more adherent target cells (CHO cells and HRBCs) were estimated. (C) Fluid-phase endocytosis. EhPL-AS- and vector-transformed cells were incubated with 2 mg/ml FITC-dextran in PBS for 30 min and subjected to quantitative estimation by spectrofluorimeter as described in Materials and Methods. The cells (right panels) were also mounted on glass slides for viewing under a fluorescent microscope (Axioscope plus; Zeiss) at 40× magnification. Some of the error bars are not visible due to small values. (*, P value < 0.05; **, P value < 0.01; ***, P value < 0.001).

key molecules involved in amoebic pathogenesis (3, 26, 34, 41, 53, 54). In this study an attempt was made to generate cell lines that have reduced levels of overall GPI-containing molecules and to correlate this reduction with functional characteristics. The approach used was to block expression of one of the early enzymes in the pathway.

At the outset the presence of GPI-Gnt complex and PIG-L activities in *E. histolytica* was demonstrated using a cell-free system. The products of these enzyme activities were susceptible to PI-PLC hydrolysis. Nitrous acid deamination revealed that one of the products (Y) contains a PI anchor with a free amine, which may have been generated through a deacetylation reaction. These products were interconvertible by acetylation and deacetylation. Thus, the data put together confirmed that products X and Y were GlcNAc-PI and GlcN-PI, respectively.

One of the ways to decipher the function of a molecule is to generate a knockout cell line or block expression of specific genes. Generating gene knockouts in *E. histolyitca* has not been possible because of the high ploidy of this organism (57). Therefore, expression blocking appears to be a better option for functional studies. Since some of the genes may be essential for proliferation, an inducible antisense approach was adopted. Such an approach utilizing the inducible tet repressor-operator system was previously shown to be useful in generating conditional expression blocking of a calcium binding protein gene of *E. histolytica* (45). In this study, in silico approaches were used to identify genes encoding the enzymes involved in the biosynthetic pathway of GPI. Since some of these genes were conserved, it was possible to find these enzymes, and one of the first enzymes, PIG-L, was used for expression blocking of the pathway by the antisense approach. The rationale for targeting one of the first enzymes is to block all types of GPI anchors and not necessarily some specific class of GPI-containing molecules.

The data presented here show that the putative PIG-L of *E. histolytica* is indeed a GlcNAc-PI-deacetylase by the following criteria. (i) EhPIG-L has 33% overall sequence identity with human PIG-L. A conserved domain is also present in EhPIG-L. (ii) *E. histolytica* cells partially blocked for PIG-L expression, when subjected to conditional tet induction, showed lower levels of deacetylase activity. Conversely, when EhPIG-L was overexpressed, the deacetylase activity was found to increase. These results demonstrated the usefulness of a system regulated by tet for conditional expression of the PIG-L gene in *E. histolytica*. (iii) The total repertoire of GPI-anchored molecules in the PIG-L-blocked cells was reduced by 85 to 90% as visualized by FLAER labeling. This was also confirmed by measuring the amount of PPG and Gal/GalNAc lectin light subunit in these cells. The antisense-inhibited cells showed a reduction in the levels of both molecules. Expression blocking of EhPIG-L resulted in partial inhibition of *E. histolytica* cell proliferation. This observation was similar to results seen with yeast and trypanosomes, where genes known to be involved in GPI anchor biosynthesis were essential for viability (16, 36).

GPI-anchored molecules are thought to participate in endocytosis (11, 27, 38, 49). Loss of endocytosis and an inhibition in adherence would reduce the pathogenic potential of *E. histolytica*. Here we showed that partial blocking of the EhPIG-L gene leads to reduction in the amoebic cell surface adhesion to target cells and a decrease in fluid phase pinocytosis. These observations are consistent with the previous finding that overexpression of a mutant form of the small subunit of Gal/GalNAc lectin lacking the GPI anchor reduced the pathogenic properties of the cells (42).

Blocking of a complete biosynthetic pathway by inhibiting a key enzyme has been achieved in many organisms (20, 39, 56). This is one of the first examples of such an approach in the protozoan parasite *E. histolytica*. This is also the first report describing some of the events in the biosynthesis of GPI anchors in *E. histolytica*.

ACKNOWLEDGMENTS

This work was partially supported by grants from the Department of Biotechnology and Department of Science & Technology, Government of India. D.V. thanks the Council for Scientific and Industrial Research and University Grants Commission, India, for a predoctoral fellowship.

We thank M.G. Low (Columbia University College of Physicians and Surgeons, New York, N.Y.) for the generous gift of bacterial PI-PLC enzyme.

REFERENCES

1. **Almeida, I. C., M. M. Camargo, D. O. Procopio, L. S. Silva, A. Mehlert, L. R. Travassos, R. T. Gazzinelli, and M. A. Ferguson.** 2000. Highly purified glycosylphosphatidylinositols from *Trypanosoma cruzi* are potent proinflammatory agents. EMBO J. **19:**1476–1485.
2. **Arya, R., A. Mehra, S. Bhattacharya, R. A. Vishwakarma, and A. Bhattacharya.** 2003. Biosynthesis of *Entamoeba histolytica* proteophosphoglycan in vitro. Mol. Biochem. Parasitol. **126:**1–8.
3. **Bhattacharya, A., R. Arya, C. G. Clark, and J. P. Ackers.** 2000. Absence of lipophosphoglycan-like glycoconjugates in *Entamoeba dispar*. Parasitology **120**(Pt. 1)**:**31–35.
4. **Bhattacharya, A., S. Bhattacharya, M. P. Sharma, and L. S. Diamond.** 1990. Metabolic labeling of *Entamoeba histolytica* antigens: characterization of a 28-kDa major intracellular antigen. Exp. Parasitol. **70:**255–263.
5. **Bhattacharya, A., R. Ghildyal, S. Bhattacharya, and L. S. Diamond.** 1990. Characterization of a monoclonal antibody that selectively recognizes a subset of *Entamoeba histolytica* isolates. Infect. Immun. **58:**3458–3461.
6. **Bhattacharya, A., R. Prasad, and D. L. Sacks.** 1992. Identification and partial characterization of a lipophosphoglycan from a pathogenic strain of *Entamoeba histolytica*. Mol. Biochem. Parasitol. **56:**161–168.
7. **Bhattacharya, S., A. Bhattacharya, and L. S. Diamond.** 1988. Comparison of repeated DNA from strains of *Entamoeba histolytica* and other *Entamoeba*. Mol. Biochem. Parasitol. **27:**257–262.
8. **Brodsky, R. A., G. L. Mukhina, S. Li, K. L. Nelson, P. L. Chiurazzi, J. T. Buckley, and M. J. Borowitz.** 2000. Improved detection and characterization of paroxysmal nocturnal hemoglobinuria using fluorescent aerolysin. Am. J. Clin. Pathol. **114:**459–466.
9. **Carver, M. A., and S. J. Turco.** 1991. Cell-free biosynthesis of lipophosphoglycan from *Leishmania donovani*. Characterization of microsomal galactosyltransferase and mannosyltransferase activities. J. Biol. Chem. **266:**10974–10981.
10. **Cheng, X. J., M. A. Hughes, C. D. Huston, B. Loftus, C. A. Gilchrist, L. A. Lockhart, S. Ghosh, V. Miller-Sims, B. J. Mann, W. A. Petri, Jr., and H. Tachibana.** 2001. Intermediate subunit of the Gal/GalNAc lectin of *Entamoeba histolytica* is a member of a gene family containing multiple CXXC sequence motifs. Infect. Immun. **69:**5892–5898.
11. **Deckert, M., M. Ticchioni, and A. Bernard.** 1996. Endocytosis of GPI-anchored proteins in human lymphocytes: role of glycolipid-based domains, actin cytoskeleton, and protein kinases. J. Cell Biol. **133:**791–799.
12. **Doering, T. L., W. J. Masterson, P. T. Englund, and G. W. Hart.** 1989. Biosynthesis of the glycosyl phosphatidylinositol membrane anchor of the trypanosome variant surface glycoprotein. Origin of the non-acetylated glucosamine. J. Biol. Chem. **264:**11168–11173.
13. **Eisenhaber, B., P. Bork, and F. Eisenhaber.** 1998. Sequence properties of GPI-anchored proteins near the omega-site: constraints for the polypeptide binding site of the putative transamidase. Protein Eng. **11:**1155–1161.
14. **Field, M. C., E. Medina-Acosta, and G. A. Cross.** 1993. Inhibition of glycosylphosphatidylinositol biosynthesis in *Leishmania mexicana* by mannosamine. J. Biol. Chem. **268:**9570–9577.
15. **Hamann, L., H. Buss, and E. Tannich.** 1997. Tetracycline-controlled gene expression in *Entamoeba histolytica*. Mol. Biochem. Parasitol. **84:**83–91.
16. **Hamburger, D., M. Egerton, and H. Riezman.** 1995. Yeast Gaa1p is required for attachment of a completed GPI anchor onto proteins. J. Cell Biol. **129:**629–639.

17. **Handman, E., and J. W. Goding.** 1985. The *Leishmania* receptor for macrophages is a lipid-containing glycoconjugate. EMBO J. **4:**329–336.
18. **Hirose, S., L. Ravi, S. V. Hazra, and M. E. Medof.** 1991. Assembly and deacetylation of *N*-acetylglucosaminyl-plasmanylinositol in normal and affected paroxysmal nocturnal hemoglobinuria cells. Proc. Natl. Acad. Sci. USA **88:**3762–3766.
19. **Houpt, E., L. Barroso, L. Lockhart, R. Wright, C. Cramer, D. Lyerly, and W. A. Petri.** 2004. Prevention of intestinal amebiasis by vaccination with the *Entamoeba histolytica* Gal/GalNac lectin. Vaccine **22:**611–617.
20. **Huang, P. L., S. N. Zhu, S. L. Lu, Z. S. Dai, and Y. L. Jin.** 2000. Inhibitor of fatty acid synthase induced apoptosis in human colonic cancer cells. World J. Gastroenterol. **6:**295–297.
21. **Katz, U., S. Ankri, T. Stolarsky, Y. Nuchamowitz, and D. Mirelman.** 2002. *Entamoeba histolytica* expressing a dominant negative *N*-truncated light subunit of its gal-lectin are less virulent. Mol. Biol. Cell **13:**4256–4265.
22. **Kucik, C. J., G. L. Martin, and B. V. Sortor.** 2004. Common intestinal parasites. Am. Fam. Physician **69:**1161–1168.
23. **Lillico, S., M. C. Field, P. Blundell, G. H. Coombs, and J. C. Mottram.** 2003. Essential roles for GPI-anchored proteins in African trypanosomes revealed using mutants deficient in GPI8. Mol. Biol. Cell **14:**1182–1194.
24. **Liu, X., and K. P. Chang.** 1992. Extrachromosomal genetic complementation of surface metalloproteinase (gp63)-deficient *Leishmania* increases their binding to macrophages. Proc. Natl. Acad. Sci. USA **89:**4991–4995.
25. **Loftus, B., I. Anderson, R. Davies, U. C. Alsmark, J. Samuelson, P. Amedeo, P. Roncaglia, M. Berriman, R. P. Hirt, B. J. Mann, T. Nozaki, B. Suh, M. Pop, M. Duchene, J. Ackers, E. Tannich, M. Leippe, M. Hofer, I. Bruchhaus, U. Willhoeft, A. Bhattacharya, T. Chillingworth, C. Churcher, Z. Hance, B. Harris, D. Harris, K. Jagels, S. Moule, K. Mungall, D. Ormond, R. Squares, S. Whitehead, M. A. Quail, E. Rabbinowitsch, H. Norbertczak, C. Price, Z. Wang, N. Guillen, C. Gilchrist, S. E. Stroup, S. Bhattacharya, A. Lohia, P. G. Foster, T. Sicheritz-Ponten, C. Weber, U. Singh, C. Mukherjee, N. M. El Sayed, W. A. Petri, Jr., C. G. Clark, T. M. Embley, B. Barrell, C. M. Fraser, and N. Hall.** 2005. The genome of the protist parasite *Entamoeba histolytica*. Nature **433:**865–868.
26. **Lushbaugh, W. B., and J. H. Miller.** 1974. Fine structural topochemistry of *Entamoeba histolytica* Schaudinn, 1903. J. Parasitol. **60:**421–433.
27. **Mayor, S., K. G. Rothberg, and F. R. Maxfield.** 1994. Sequestration of GPI-anchored proteins in caveolae triggered by cross-linking. Science **264:** 1948–1951.
28. **McConville, M. J., and M. A. Ferguson.** 1993. The structure, biosynthesis and function of glycosylated phosphatidylinositols in the parasitic protozoa and higher eukaryotes. Biochem. J. **294**(Pt. 2)**:**305–324.
29. **McCoy, J. J., B. J. Mann, T. S. Vedvick, Y. Pak, D. B. Heimark, and W. A. Petri, Jr.** 1993. Structural analysis of the light subunit of the *Entamoeba histolytica* galactose-specific adherence lectin. J. Biol. Chem. **268:**24223–24231.
30. **McCoy, J. J., B. J. Mann, T. S. Vedvick, and W. A. Petri, Jr.** 1993. Sequence analysis of genes encoding the light subunit of the *Entamoeba histolytica* galactose-specific adhesin. Mol. Biochem. Parasitol. **61:**325–328.
31. **McCoy, J. J., A. M. Weaver, and W. A. Petri, Jr.** 1994. Use of monoclonal anti-light subunit antibodies to study the structure and function of the *Entamoeba histolytica* Gal/GalNAc adherence lectin. Glycoconj. J. **11:**432–436.
32. **McNeely, T. B., and S. J. Turco.** 1990. Requirement of lipophosphoglycan for intracellular survival of *Leishmania donovani* within human monocytes. J. Immunol. **144:**2745–2750.
33. **Mensa-Wilmot, K., N. Garg, B. S. McGwire, H. G. Lu, L. Zhong, D. A. Armah, J. H. LeBowitz, and K. P. Chang.** 1999. Roles of free GPIs in amastigotes of *Leishmania*. Mol. Biochem. Parasitol. **99:**103–116.
34. **Moody, S., S. Becker, Y. Nuchamowitz, and D. Mirelman.** 1997. Virulent and avirulent *Entamoeba histolytica* and *E. dispar* differ in their cell surface phosphorylated glycolipids. Parasitology **114**(Pt. 2)**:**95–104.
35. **Moody-Haupt, S., J. H. Patterson, D. Mirelman, and M. J. McConville.** 2000. The major surface antigens of *Entamoeba histolytica* trophozoites are GPI-anchored proteophosphoglycans. J. Mol. Biol. **297:**409–420.
36. **Nagamune, K., T. Nozaki, Y. Maeda, K. Ohishi, T. Fukuma, T. Hara, R. T. Schwarz, C. Sutterlin, R. Brun, H. Riezman, and T. Kinoshita.** 2000. Critical roles of glycosylphosphatidylinositol for *Trypanosoma brucei*. Proc. Natl. Acad. Sci. USA **97:**10336–10341.
37. **Nakamura, N., N. Inoue, R. Watanabe, M. Takahashi, J. Takeda, V. L. Stevens, and T. Kinoshita.** 1997. Expression cloning of PIG-L, a candidate *N*-acetylglucosaminyl-phosphatidylinositol deacetylase. J. Biol. Chem. **272:** 15834–15840.
38. **Parton, R. G., B. Joggerst, and K. Simons.** 1994. Regulated internalization of caveolae. J. Cell Biol. **127:**1199–1215.
39. **Pekala, P. H., M. Kawakami, C. W. Angus, M. D. Lane, and A. Cerami.** 1983. Selective inhibition of synthesis of enzymes for de novo fatty acid biosynthesis by an endotoxin-induced mediator from exudate cells. Proc. Natl. Acad. Sci. USA **80:**2743–2747.
40. **Petri, W. A., Jr.** 2002. Pathogenesis of amebiasis. Curr. Opin. Microbiol. **5:**443–447.
41. **Prasad, R., M. Tola, S. Bhattacharya, M. P. Sharma, and A. Bhattacharya.** 1992. Recognition of *Entamoeba histolytica* lipophosphoglycan by a strain-specific monoclonal antibody and human immune sera. Mol. Biochem. Parasitol. **56:**279–287.
42. **Ramakrishnan, G., S. Lee, B. J. Mann, and W. A. Petri, Jr.** 2000. *Entamoeba histolytica*: deletion of the GPI anchor signal sequence on the Gal/GalNAc lectin light subunit prevents its assembly into the lectin heterodimer. Exp. Parasitol. **96:**57–60.
43. **Ravdin, J. I., and R. L. Guerrant.** 1981. Role of adherence in cytopathogenic mechanisms of *Entamoeba histolytica*. Study with mammalian tissue culture cells and human erythrocytes. J. Clin. Investig. **68:**1305–1313.
44. **Saffer, L. D., and W. A. Petri, Jr.** 1991. Role of the galactose lectin of *Entamoeba histolytica* in adherence-dependent killing of mammalian cells. Infect. Immun. **59:**4681–4683.
45. **Sahoo, N., S. Bhattacharya, and A. Bhattacharya.** 2003. Blocking the expression of a calcium binding protein of the protozoan parasite *Entamoeba histolytica* by tetracycline regulatable antisense-RNA. Mol. Biochem. Parasitol. **126:**281–284.
46. **Sambrook, J., E. F. Fritsch, and T. Maniatis.** 1989. Molecular cloning: a laboratory manual, 2nd ed. Cold Spring Harbor Laboratory Press, Cold Spring Harbor, N.Y.
47. **Schofield, L., M. C. Hewitt, K. Evans, M. A. Siomos, and P. H. Seeberger.** 2002. Synthetic GPI as a candidate anti-toxic vaccine in a model of malaria. Nature **418:**785–789.
48. **Schofield, L., S. Novakovic, P. Gerold, R. T. Schwarz, M. J. McConville, and S. D. Tachado.** 1996. Glycosylphosphatidylinositol toxin of *Plasmodium* upregulates intercellular adhesion molecule-1, vascular cell adhesion molecule-1, and E-selectin expression in vascular endothelial cells and increases leukocyte and parasite cytoadherence via tyrosine kinase-dependent signal transduction. J. Immunol. **156:**1886–1896.
49. **Skretting, G., M. L. Torgersen, B. van Deurs, and K. Sandvig.** 1999. Endocytic mechanisms responsible for uptake of GPI-linked diphtheria toxin receptor. J. Cell Sci. **112**(Pt. 22)**:**3899–3909.
50. **Smith, P. K., R. I. Krohn, G. T. Hermanson, A. K. Mallia, F. H. Gartner, M. D. Provenzano, E. K. Fujimoto, N. M. Goeke, B. J. Olson, and D. C. Klenk.** 1985. Measurement of protein using bicinchoninic acid. Anal. Biochem. **150:**76–85.
51. **Spath, G. F., L. A. Garraway, S. J. Turco, and S. M. Beverley.** 2003. The role(s) of lipophosphoglycan (LPG) in the establishment of *Leishmania major* infections in mammalian hosts. Proc. Natl. Acad. Sci. USA **100:**9536–9541.
52. **Spath, G. F., L. F. Lye, H. Segawa, D. L. Sacks, S. J. Turco, and S. M. Beverley.** 2003. Persistence without pathology in phosphoglycan-deficient *Leishmania major*. Science **301:**1241–1243.
53. **Srivastava, G., M. T. Anand, S. Bhattacharya, and A. Bhattacharya.** 1995. Lipophosphoglycan is present in distinctly different form in different *Entamoeba histolytica* strains and absent in *Entamoeba moshkovskii* and *Entamoeba invadens*. J. Eukaryot. Microbiol. **42:**617–622.
54. **Stanley, S. L., Jr., H. Huizenga, and E. Li.** 1992. Isolation and partial characterization of a surface glycoconjugate of *Entamoeba histolytica*. Mol. Biochem. Parasitol. **50:**127–138.
55. **Stevens, V. L., H. Zhang, and M. Harreman.** 1996. Isolation and characterization of a Chinese hamster ovary (CHO) mutant defective in the second step of glycosylphosphatidylinositol biosynthesis. Biochem. J. **313**(Pt. 1)**:**253–258.
56. **Surolia, N., and A. Surolia.** 2001. Triclosan offers protection against blood stages of malaria by inhibiting enoyl-ACP reductase of *Plasmodium falciparum*. Nat. Med. **7:**167–173.
57. **Tannich, E., I. Bruchhaus, R. D. Walter, and R. D. Horstmann.** 1991. Pathogenic and nonpathogenic *Entamoeba histolytica*: identification and molecular cloning of an iron-containing superoxide dismutase. Mol. Biochem. Parasitol. **49:**61–71.
58. **Vidugiriene, J., and A. K. Menon.** 1993. Early lipid intermediates in glycosylphosphatidylinositol anchor assembly are synthesized in the ER and located in the cytoplasmic leaflet of the ER membrane bilayer. J. Cell Biol. **121:**987–996.
59. **Vidugiriene, J., and A. K. Menon.** 1994. The GPI anchor of cell-surface proteins is synthesized on the cytoplasmic face of the endoplasmic reticulum. J. Cell Biol. **127:**333–341.
60. **Vines, R. R., J. E. Purdy, B. D. Ragland, J. Samuelson, B. J. Mann, and W. A. Petri, Jr.** 1995. Stable episomal transfection of *Entamoeba histolytica*. Mol. Biochem. Parasitol. **71:**265–267.
61. **Watanabe, R., Y. Murakami, M. D. Marmor, N. Inoue, Y. Maeda, J. Hino, K. Kangawa, M. Julius, and T. Kinoshita.** 2000. Initial enzyme for glycosylphosphatidylinositol biosynthesis requires PIG-P and is regulated by DPM2. EMBO J. **19:**4402–4411.

Editor: W. A. Petri, Jr.